2023-11-30

Cryptic bacterial pathogens of diatoms peak during senescence of a winter diatom bloom

Branscombe, L

10.1111/nph.19441
New Phytologist
Wiley

New Phytologist

Research

Cryptic bacterial pathogens of diatoms peak during senescence of a winter diatom bloom

Laura Branscombe[1,2], Ellen L. Harrison[1,3], Zhi Yi Daniel Choong[1,2], Courtney Swink[1,3], Matthew Keys[1], Claire Widdicombe[4], William H. Wilson[1,2], Michael Cunliffe[1,2] and Katherine Helliwell[1,3]

[1]Marine Biological Association, Citadel Hill, Plymouth, PL1 2PB, UK; [2]School of Biological and Marine Sciences, University of Plymouth, Plymouth, PL4 8AA, UK; [3]Biosciences, Faculty of Health and Life Sciences, University of Exeter, Exeter, EX4 4QD, UK; [4]Plymouth Marine Laboratory, Prospect Place, Plymouth, PL1 3DH, UK

Author for correspondence:
Katherine Helliwell
Email: k.helliwell@exeter.ac.uk; katherine.helliwell@mba.ac.uk

Received: *12 July 2023*
Accepted: *27 October 2023*

New Phytologist (2023)
doi: 10.1111/nph.19441

Key words: algicidal, *Coscinodiscus*, diatom–bacteria interactions, diatoms, plaque assay, *Ponticoccus*.

Summary

- Diatoms are globally abundant microalgae that form extensive blooms in aquatic ecosystems. Certain bacteria behave antagonistically towards diatoms, killing or inhibiting their growth. Despite their crucial implications to diatom bloom and population health, knowledge of diatom antagonists in the environment is fundamentally lacking.
- We report systematic characterisation of the diversity and seasonal dynamics of bacterial antagonists of diatoms via plaque assay sampling in the Western English Channel, where diatoms frequently bloom. Unexpectedly, peaks in detection did not occur during characteristic spring diatom blooms, but coincided with a winter bloom of *Coscinodiscus*, suggesting that these bacteria likely influence distinct diatom host populations.
- We isolated multiple bacterial antagonists, spanning 4 classes and 10 bacterial orders. Notably, a diatom attaching Roseobacter *Ponticoccus alexandrii* was isolated multiple times, indicative of a persistent environmental presence. Moreover, many isolates had no prior reports of antagonistic activity towards diatoms. We verified diatom growth inhibitory effects of eight isolates. In all cases tested, these effects were activated by pre-exposure to diatom organic matter. Discovery of widespread 'cryptic' antagonistic activity indicates that bacterial pathogenicity towards diatoms is more prevalent than previously recognised.
- Finally, examination of the global biogeography of WEC antagonists revealed co-occurrence patterns with diatom host populations in marine waters globally.

Introduction

Diatoms are single-celled photosynthetic eukaryotes that contribute *c.* 40% of marine primary productivity (Armbrust, 2009). Diatoms frequently form large, sometimes toxic blooms, during which they can constitute up to 90% of the phytoplankton community (Han & Furuya, 2000). Organic matter produced during a bloom is vital for sustaining planktonic life (Buchan *et al.*, 2014). Biomass that is not recycled can form nutrient-rich aggregates that sink to the sea floor, sequestering carbon in the deep ocean (Jiao *et al.*, 2010). It is thus crucial to understand environmental drivers controlling diatom bloom dynamics. A range of abiotic (e.g. nutrients, light, and temperature) and biotic (e.g. grazers and viruses) factors control bloom formation and demise (Buchan *et al.*, 2014). However, the relative contribution of these drivers, and the spectrum of biotic pressures influencing phytoplankton populations in the ocean, remains open to debate (Buchan *et al.*, 2014). Given that around half of the carbon that is fixed by phytoplankton such as diatoms is processed by bacteria (Cole *et al.*, 1988; Ducklow *et al.*, 1993), gaining insight into the interactions between diatoms and bacteria and their influence on natural bloom dynamics is crucial for better understanding nutrient fluxes and the fate of carbon in the oceans.

Diatoms engage in a suite of biotic interactions with bacteria, ranging from synergistic to antagonistic (Mayali & Azam, 2004; Amin *et al.*, 2012). Accumulating evidence indicates that diatoms host species-specific bacterial communities, a so-called 'diatom microbiome' (Amin *et al.*, 2012; Helliwell *et al.*, 2022). Bacterial taxa typically belonging to *Alphaproteobacteria*, *Bacteroidetes*, and *Gammaproteobacteria* are frequently associated with diatoms (Schäfer *et al.*, 2002; Grossart *et al.*, 2005), with certain genera in particular (e.g. *Sulfitobacter*, *Roseobacter*, *Alteromonas*, and *Flavobacterium*) most commonly identified (Amin *et al.*, 2012). Notably, several interactions between diatoms and members of the *Rhodobacteraceae* (of the *Alphaproteobacteria*) are synergistic (Hünken *et al.*, 2008; Amin *et al.*, 2015; Durham *et al.*, 2015; Suleiman *et al.*, 2016), with bacteria conferring protection against environmental stressors (e.g. oxidative stress Hünken *et al.*, 2008) and/or alleviating the demands of diatoms for nutrients such as vitamins (Durham *et al.*, 2015) and nitrogen (Amin *et al.*, 2015; Suleiman *et al.*, 2016).

Certain bacteria also have algicidal (causing cell death) and/or algistatic (growth inhibitory) effects against diatoms (Mayali &

Azam, 2004; Meyer *et al.*, 2017). These antagonistic bacteria tend to belong to the *Gammaproteobacteria* (Coyne *et al.*, 2022), specifically of the orders *Alteromonadales* and *Pseudomonadales*, as well as *Flavobacteria* (Mayali & Azam, 2004). Current understanding of the mechanistic basis of antagonistic diatom–bacteria interactions has been yielded largely through the study of culture-based model systems. For instance, the Flavobacterium *Kordia algicida* displays algicidal activities against the diatoms *Thalassiosira weissflogii*, *Phaeodactylum tricornutum*, and *Skeletonema costatum* (Paul & Pohnert, 2011), via release of extracellular proteases that cause diatom cell lysis (Paul & Pohnert, 2011). Another Flavobacterium, *Croceibacter atlanticus*, is also capable of inhibiting the growth of various diatoms, but to different extents (Van Tol *et al.*, 2017). Laboratory study demonstrated that *C. atlanticus* directly attaches to diatoms and inhibits cell division. Moreover, *C. atlanticus* exudates caused increases in intra- and extracellular carbon in *Thalassiosira pseudonana*, suggesting that bacterial antagonists can modulate host metabolism to support their growth (Bartolek *et al.*, 2022).

While model systems have been instrumental in elucidating the impacts of algicidal bacteria on diatom physiology, insights of the dynamics and nature of diatom algicidal bacteria in natural marine ecosystems is fundamentally lacking. This is in part due to limitations in isolation and detection, with strains typically being identified from nonaxenic algal cultures (Amin *et al.*, 2015; Van Tol *et al.*, 2017) or collected *ad hoc* (Coyne *et al.*, 2022). These factors have limited knowledge of diatom antagonists in the environment, and many open questions remain. For instance, the prevalence and diversity of bacterial antagonists that co-occur with diatoms remains unknown. This, coupled with knowledge of the host range of antagonists towards diatoms and host susceptibility to different bacteria inhabiting the same ecosystem, is necessary to better understand the ecological relevance of bacterial antagonists. Gaining insights into their seasonal dynamics is also necessary to explore co-occurrences with host species. Finally, we have little knowledge of how broadly distributed bacterial antagonists are in marine ecosystems globally. To address these questions, a more systematic ecosystem approach is necessary to characterise the bacterial 'pathobiome' of diatoms in nature.

The Western Channel Observatory (WCO) is one of the most comprehensive oceanographic time series in the world, collecting plankton abundance data weekly throughout the year (Widdicombe *et al.*, 2010). Diatoms can dominate Western English Channel (WEC) phytoplankton communities, with spring blooms frequently made up of *Chaetoceros*, *Thalassiosira*, and *Skeletonema* (Widdicombe *et al.*, 2010). Peaks of certain diatoms during winter months are also well documented (Gomez & Souissi, 2010; Arsenieff *et al.*, 2020). Western English Channel (WEC) bacterial communities also exhibit robust seasonal patterns (Gilbert *et al.*, 2009, 2012). *Alphaproteobacteria*, namely *Rickettsiales* (SAR11) and *Rhodobacterales*, constitute the most abundant taxa, in addition to *Flavobacteriales* (*Bacteroidetes*), and *Gammaproteobacteria* (*Vibrionales* and *Pseudomonadales*; Gilbert *et al.*, 2012). Notably, abundances of *Flavobacteriale* and *Rhodobacterale* populations correlated significantly with phytoplankton-derived polysaccharides during a spring WEC diatom bloom (Taylor & Cunliffe, 2016), suggesting tight coupling of bacterial population structure and bloom succession. The accessibility of the WEC off the coast of Plymouth lends itself to routine studies that have been invaluable for the identification of interactions between planktonic groups. For instance, relationships between WEC diatoms and mycoplankton have been revealed through the detection of concurrent diatom and chytrid blooms observed interannually in the WEC (Taylor *et al.*, 2014). Additionally, single-cell picking approaches led to the isolation of a novel thraustochytrid 'ThrauL4' that parasitises *Chaetoceros* (Laundon *et al.*, 2021).

These studies highlight the power of long-term monitoring coupled with environmental sampling approaches that 'bring-into-the-laboratory' biotic associations representative of those in nature. Here, we exploit our unique access to WEC microbial communities to systematically assess the diversity of bacterial antagonists of diatoms in the WEC. Utilising a plaque assay approach (Yamamoto, 1978) over the course of an annual cycle, we have characterised the diversity and physiological traits of the bacterial 'pathobiome' of bloom-forming diatoms residing in the WEC. Our study uncovers seasonal patterns of previously unreported antagonistic activity against diatoms in a diverse range of bacterial lineages.

Materials and Methods

Algal strains and culture conditions

The diatoms *Thalassiosira pseudonana* (PLY693; CCMP1335), *Thalassiosira weissflogii* (PLY541), *Skeletonema* sp. (PLY627), *Chaetoceros* sp. (PLY617), *Phaeodactylum tricornutum* (PLY100), (as well as the coccolithophore *Isochrysis galbana* (PLY565) and dinoflagellate *Amphidinium carterae* (PLY450)) were obtained from the Marine Biological Association Culture Collection (Plymouth, UK; Supporting Information Table S1; Fig. S1A). *Coscinodiscus wailesii* was isolated during this study from the WEC. As *Skeletonema* sp. (PLY627) and *Chaetoceros* sp. (PLY617) were identified only to genus level, 18S rRNA gene sequences were amplified via PCR using the primers Euk1A (CTGGTTGAT CCTGCCAG) and EUKB (TGATCCTTCTGCAGGTTCA CCTAC), and sequences are given in Dataset S1. All algae were cultured in filtered WEC seawater supplemented with f/2 nutrients (including Na_2SiO and vitamins; Guillard & Ryther, 1962), at 18°C (15°C for *C. wailesii*) under a 16 h : 8 h, light : dark cycle with a light intensity of 30–80 μmol m^2 s^{-1}.

Isolation of *Coscinodiscus wailesii*

Coscinodiscus wailesii cells were isolated from a natural phytoplankton population on 17 October 2022. Seawater was collected with a plankton net (200 μm mesh size) deployed at a depth of 5 m in the Plymouth Sound, WEC (50°20′0.093″N, 4°08′0.915″W). *C. wailesii* cells were isolated with a micropipette prepared on a P-97 micropipette puller with a tip diameter of *c.* 350 μm (Sutter, Novato, CA, USA). Cells were washed by

resuspension into 1 ml droplets of sterile seawater three times before being placed into aged filtered sterile seawater with f/2 medium with 100 µM silicate, in 4-ml well plates (*c.* 10 cells per well).

Antibiotic treatment of diatom cultures and verification of axenity

All diatom strains used for this study were treated with a cocktail of antibiotics before experimentation. Treatment consisted of three sequential rounds (with the exception of *C. wailesii* that only had one treatment round) of 3-d incubations of diatom cells in f/2 medium supplemented with 0.7 mg ml^{-1} ampicillin, 0.1 mg ml^{-1} streptomycin, and 0.5 mg ml^{-1} penicillin. Treated diatoms were subsequently subcultured into fresh f/2 medium without antibiotics and allowed to reach exponential growth phase. To check the axenity of the cultures, a sample of cells was stained with the nucleic acid–specific stain Hoechst (1 µl ml^{-1}), incubated in the dark for 30 min at 20°C in a glass-bottomed dish, and viewed under epifluorescent illumination (excitation at 395 nm and emission at 460 nm) using a Leica DMi8 inverted microscope (Leica Microsystems, Milton Keynes, UK) with a 63 × 1.4 NA oil immersion objective. Bacteria were clearly visible in nontreated control cultures but were not seen in the antibiotic-treated cultures used in this study. Cultures were checked frequently (approximately monthly) via epifluorescence staining and plating on Difco Marine Broth plates through the course of the study. On occasions when contamination was detected, cells were retreated with antibiotics and visually inspected as described previously. While antibiotic treatment of *C. wailesii* substantially reduced bacterial load, we did not obtain a completely axenic culture, due to the sensitivity of this strain to antibiotics.

Isolation of antagonistic bacteria from the Western English Channel via plaque assays

Axenic diatom host species were cultured under standard conditions for 14 d for use in plaque assays. For each assay, 100 ml of diatom cells was concentrated by centrifugation at 2740 ***g*** for 10 min and cell pellets were resuspended in 500 µl sterile f/2 medium. For the bacterial inoculum from the WEC, surface water (5 m) samples were collected monthly (where possible) from Station L4 (50°15.00′N, 4°13.02′W, Fig. S1B) in 20 l carboys. For the June 2020 sample, it was not possible for the research vessel to go to sea for logistical reasons (COVID-19 pandemic), instead samples were taken off the coast of Plymouth (50.363338, −4.139739). Seawater (1 l) was sequentially filtered through 100, 40, and 10 µm pluristrainers to remove larger eukaryotic cells and debris (capturing free-living bacteria as well as bacteria associated with smaller (< 10 µm) diatom cells). Finally, remaining cells were collected on a 0.22 µm membrane. The membrane was subsequently washed with 1 ml of sterile seawater to produce a concentrated filtrate of bacterial cells.

To prepare plaque assays, 100 µl of bacterial filtrate (or autoclaved filtered seawater for the control) was inoculated into 500 µl of the concentrated 14-d-old axenic diatom culture and left to incubate at room temperature for 30 min to 1 h. The diatom-bacteria co-culture was added to 4.4 ml of 0.4% molten (55°C) f/2 agar (f/2 medium supplemented with 0.4 g l^{-1} agarose) and mixed thoroughly by inversion. Agar was poured immediately onto a 1% f/2 agar plate, incubated at 18°C under a 16 h : 8 h, light : dark cycle with a light intensity of 50–80 µmol m^{-2} s^{-1}, and observed for several weeks for plaque formation.

For the plaque-to-plaque assay experiments described in Table S2, upon plaque formation on the original plaque assay plate, single plaques were picked with a sterile loop and immediately used to create a new inoculum by placing into 500 µl sterile seawater, 100 µl of which was inoculated into a fresh plaque assay with each of the diatom hosts.

Identification of bacterial isolates from plaque assays

To isolate and identify bacteria, plaques picked from successful plaque assays were streaked onto 1% agar plates made up of ½ Yeast Tryptone Sea Salts (YTSS) medium (containing 2 g l^{-1} of yeast extract, 1.25 g l^{-1} of tryptone, and 20 g l^{-1} of sea salts (Sigma)). Pure cultures were obtained by streaking single colonies a minimum of four times. In instances where two colony types were apparent from a plaque streak out (P45, P47, P46, P49, and P29; Fig. S2), both colonies were processed and sequenced. Bacterial 16S rRNA gene was amplified via a GoTaq (Promega) colony PCR using primers 27f (5′-AGAGTTTGATCMTGG CTCAG-3′) and 1492r (5′-TACGGYTACCTTGTTACG ACTT-3′; Lane *et al.*, 1985; Turner *et al.*, 1999), and the following PCR cycle conditions: initial denaturation at 95°C for 5 min, followed by 32 cycles of (1) denaturation at 95°C for 30 s, (2) annealing at 50.1°C for 30 s, and (3) extension at 72°C for 90 s. A final extension at 72°C was then carried out for 5 min. 16S rRNA PCR products were purified using a QIAquick PCR Purification kit (Qiagen) and sequenced via Sanger sequencing by Source Bioscience (Cambridge, UK). Retrieved sequences were trimmed and aligned using MEGA11 (Tamura *et al.*, 2021), and closest hits were identified using the NCBI Basic Local Alignment Search Tool (BLAST) nucleotide database (Sayers *et al.*, 2022). The phylogenetic classification of hits was then validated via construction of maximum likelihood trees with type strains from the relevant genera obtained via the ribosomal Database Project (Methods S1).

Physiological growth assays co-culturing diatoms with WEC bacteria

Before inoculation of co-culture experiments, bacteria were pregrown for 4 d at 18°C on ½YTSS medium or Dead Diatom Medium (DDM) agar plates. DDM plates were prepared by autoclaving 14-d-old axenic diatom cultures with 1% agarose and used the same day. For all experiments, DDM was prepared from the diatom host the bacterium was to be inoculated into co-culture with (i.e. *T. pseudonana* DDM for *T. pseudonana-Ponticoccus alexandrii* co-cultures). Except for *C. wailesii–P. alexandrii* experiments

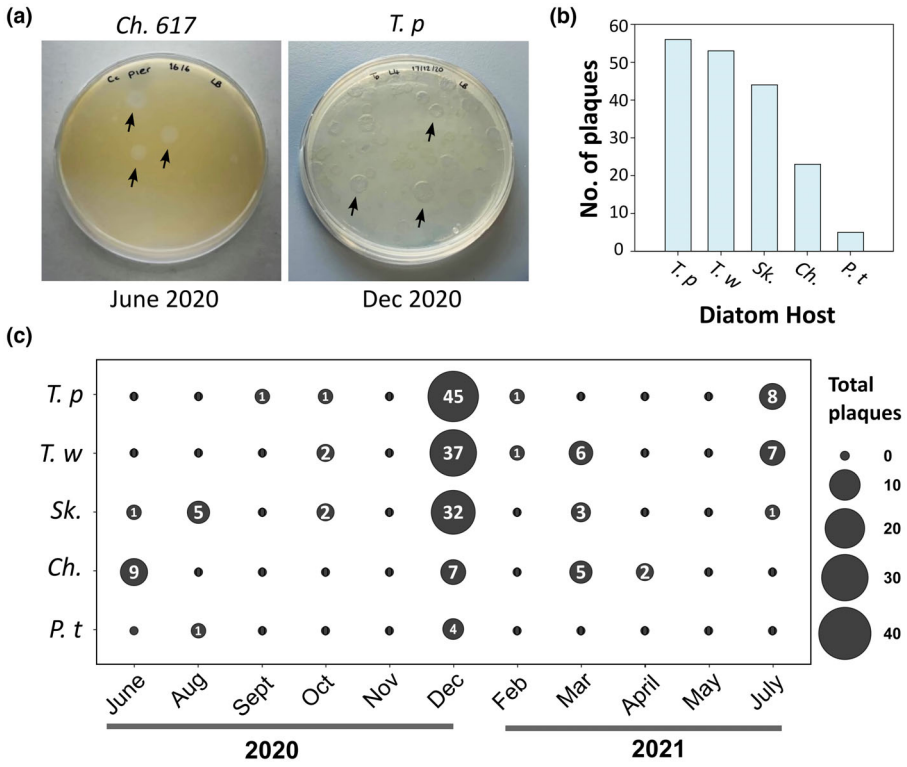

Fig. 1 Systematic isolation of naturally occurring diatom antagonists in the Western English Channel. (a) Photographs of an example *Chaetoceros* sp. PLY617 (*Ch*. 617) and *Thalassiosira pseudonana* (*T. p*) plaque assay plate from June 2020 and December 2020, respectively. Several clearance plaques are indicated (black arrows). (b) Total number of plaques obtained for each diatom host over the 13-month sampling period, including for *T. p*, *Thalassiosira weissflogii* (*T. w*), *Skeletonema* sp. PLY617, *Ch*. 617 (*Ch*.), as well as *Phaeodactylum tricornutum* (*P. t*). (c) Bubble plot showing the number of plaques observed per diatom host each sampling month.

in which *P. alexandrii* was pregrown on *T. pseudonana* DDM plates. Bacteria pregrown on ½YTSS or DDM plates were collected with a sterile loop and resuspended in 1 ml (0.2 µm) filtered seawater without nutrients. This bacterial suspension was inoculated into fresh f/2 medium to a final optical density (OD)600 of 0.01, unless stated otherwise. Host diatoms were inoculated to a concentration of 30 000 cells ml^{-1} (with the exception of *C. wailesii* where the starting density was 8 cells ml^{-1}). Diatom cell density was measured during exponential phase of diatom growth using a haemocytometer (or Sedgewick Rafter cell for *C. wailesii*), and maximum quantum efficiency of photosystem II (F_v/F_m) monitored using a PSI AquaPen AP100 (Photon Systems Instruments, Drasov, Czech Republic). For experiments determining viability of *T. pseudonana* cells in co-culture with *P. alexandrii*, bacterial cells were pregrown on liquid *T. pseudonana* DDM + 0.1% glucose before being inoculated into co-culture. Diatom cell counts were taken using a Luna Automated Cell counter (Logos Biosystems, Villeneuve-d'Ascq, France), using SYTOX Green stain NucGreen™ Dead 488 (Thermo Fisher Scientific, Paisley, UK).

Results

A systematic environmental pipeline to isolate naturally occurring diatom antagonists

Exploiting routine access to WEC microbial communities, we developed a systematic environmental sampling pipeline to isolate bacterial antagonistis of diatoms, employing a soft-agar-overlay plaque assay technique. This entailed inoculating concentrated suspensions of five diatom hosts with the bacterial fraction of WEC seawater (the 'Materials and Methods' section; Fig. S1), with appearance of regions of clearance or 'plaques' on the diatom lawns indicative of diatom growth inhibition. Diatoms chosen for this study included four centric diatoms: *T. pseudonana* (PLY693), *T. weissflogii* (PLY541), *Skeletonema* sp. PLY627, and *Chaetoceros* sp. PLY617, alongside the model pennate *P. tricornutum* (PLY100; Table S1). Several of these cultures were originally isolated from the WEC, and all are documented to inhabit WEC waters, with *Thalassiosira*, *Skeletonema*, and *Chaetoceros* representing some of the most abundant diatom genera in the WEC (Widdicombe *et al.*, 2010) and indeed globally (Malviya *et al.*, 2016). While we never observed plaques on control assay plates (inoculated with autoclaved seawater), plaques were frequently observed on assays inoculated with the bacterial fraction of seawater (Fig. 1a). In total, across the five diatom hosts and over 13 months of sampling, we observed 181 plaques. The greatest number were obtained on planktonic centric diatoms, with *T. pseudonana* being the most 'susceptible' host having 56 plaques observed in total, followed by *T. weissflogii* (53 plaques), *Skeletonema* sp. PL7627 (44 plaques), and *Chaetoceros* sp. PLY617 (23 plaques; Fig. 1b). By comparison, only five plaques were isolated on the benthic pennate *P. tricornutum*. The number of plaques observed per month also varied, with values ranging from none (November 2020 and May 2021) to over a hundred across the five diatom hosts (December 2020; Fig. 1c).

Recurrent isolation of diverse WEC plaque-associated bacteria spanning 4 classes and 10 orders of bacterial diversity

Bacteria were isolated from individual plaques by streaking single colonies a minimum of four times and subsequently identifying

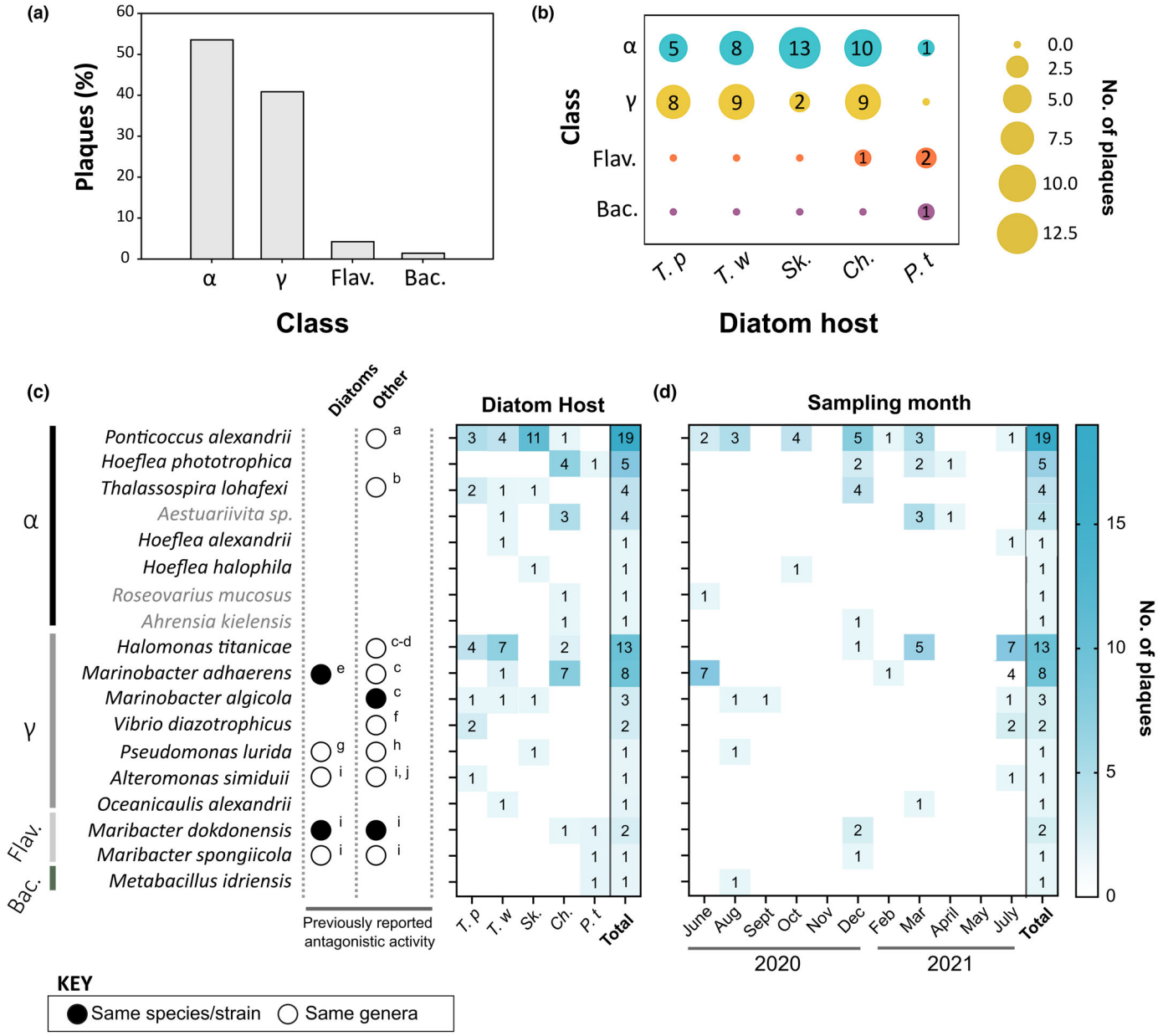

Fig. 2 Recurrent isolation of diverse bacteria from plaque assays on different diatom hosts and sampling months. (a) Percentage of plaques identified to contain bacteria belonging to the classes *Alphaproteobacteria* (α), *Gammaproteobacteria* (γ), *Flavobacteria* (Flav.), and *Bacilli* (Bac.), respectively. (b) Bubble plot showing the number of plaques identified containing bacteria belonging to each bacterial class per diatom host species. (c) Heat map showing the no. of plaques for each WEC bacterial isolate across different diatom hosts. Those species that have previously been reported to confer antagonistic activity against diatoms and/or other eukaryotic phytoplankton are indicated, with the relevant literature cited as follows: [a]Chi *et al*. (2017), [b]Lu *et al*. (2016), [c]Zheng *et al*. (2018), [d]Dungca-Santos *et al*. (2019), [e]Deng *et al*. (2022), [f]Li *et al*. (2014), [g]Kim *et al*. (2018), [h]Aiyar *et al*. (2017), [i]Wang *et al*. (2016), [j]Shi *et al*. (2018). Bacterial classes are also labelled. Three strains (coloured grey) could not be maintained following their isolation and cultures are therefore not available (the 'Materials and Methods' section). (d) Heatmap of no. of plaques identified per bacterium each sampling month. For the December 2020 sampling point, there were more plaques (125) than could be identified.

the bacteria via 16S rRNA gene sequencing (the 'Materials and Methods' section). This was done for each plaque obtained during the sampling, with the exception of December 2020, for which three plaques per host were randomly selected, as the number of plaques (125) was too great to process. In a total of 65 plaques identified, 18 different bacterial species were identified, spanning 4 classes and 10 orders of bacteria (Fig. S2; Dataset S2).

In some instances, more than one bacterium was identified from a plaque (plaques P29, P45, P47, P46, and P49; Fig. S2). Bacteria belonging to the *Alphaproteobacteria* were most frequently identified (over 50% of plaques), followed by *Gammaproteobacteria* (40.8%), *Flavobacteria* (4.2%), and least frequently were bacterial species belonging to the class *Bacilli* (1.4%; Fig. 2a). We found that *Alphaproteobacteria* were most frequently isolated

from plaque assays with the centric diatoms *Skeletonema* sp. PLY627 and *Chaetoceros* sp. PLY617 (Fig. 2b). By comparison, *Gammaproteobacteria* were detected least frequently on *Skeletonema* sp. PLY627, being detected predominantly on the *Thalassiosira* species alongside *Chaetoceros* sp. PLY617. Notably, certain bacterial species were isolated on multiple independent occasions. For instance, the *Roseobacter P. alexandrii* (*Alphaproteobacteria*) was detected on 19 independent occasions on seven sampling months, and across all four centric diatom hosts, but not *P. tricornutum* (Fig. 2c,d). The *Gammaproteobacteria H. titanicae* and *M. adhaerens* were detected the second and third most frequently, being identified in 13 and 8 plaques, respectively.

To determine whether any of our isolates had prior reports of being algicidal, we conducted a literature review. This revealed that antagonistic activity against algae has been reported previously in eight of the genera of the WEC isolates, including *Ponticoccus* (Chi *et al.*, 2017), *Thalassospira* (Lu *et al.*, 2016), *Halomonas* (Zheng *et al.*, 2018), *Marinobacter* (Zheng *et al.*, 2018; Deng *et al.*, 2022), *Vibrio* (Li *et al.*, 2014), *Pseudomonas* (Aiyar *et al.*, 2017; Kim *et al.*, 2018), *Alteromonas* (Wang *et al.*, 2016; Shi *et al.*, 2018), and *Maribacter* (Wang *et al.*, 2016; Fig. 2c). This was to species level for three bacteria (*Marinobacter algicola*, *Marinobacter adhaerens* and *Maribacter dokdonensis*). Of the WEC isolates, prior reports of antagonistic behaviour towards diatoms have been reported only for *Pseudomonas* (Kim *et al.*, 2018), *Alteromonas* (Wang *et al.*, 2016) species, and *M. dokdonensis* (Wang *et al.*, 2016).

Seasonally persistent *P. alexandrii* exhibits facultative algicidal activity against diatoms in a species-specific manner

Closer inspection of plaques clearly showed clearance of diatom cells (Fig. S3), indicating that the bacterial isolates from plaques likely confer a growth inhibitory and/or algicidal effect towards diatoms. To further investigate the effect of WEC plaque-forming bacteria, we conducted a range of experiments in both plaque assay and liquid culture. To focus these investigations, we examined the most frequently isolated bacterium, *P. alexandrii*. To verify that plaques from which *P. alexandrii* was isolated could recapitulate plaque formation on diatom plates, we inoculated material from dissected plaques into fresh plaque assays. These 'plaque-to-plaque' assays resulted in the formation of numerous new plaques on *T. pseudonana*, *Skeletonema* sp. PLY627, and *Chaetoceros* sp. PLY617, but not *T. weissflogii* or *P. tricornutum* plates (Table S2). Incidentally, we could also propagate plaques identified to contain *M. adhaerens* and *M. algicola* in this manner. We therefore tested whether pure cultures of *P. alexandrii* could cause plaque formation. Repeated trials inoculating *P. alexandrii* pregrown on ½YTSS agar plates into *T. pseudonana* plaque assays failed to recapitulate plaque formation. Since the plaque-to-plaque assays successfully yielded plaque formation, we postulated that *P. alexandrii* cells growing on diatom soft-overlay plates are in a different physiological state to cells grown on ½YTSS medium. To test the plaque-forming ability of *P. alexandrii* cells grown in conditions more akin to those within a plaque, we tested *P. alexandrii* cells pregrown on medium made up of autoclaved diatom cultures, hereafter 'Dead Diatom Medium' (DDM). Inoculation of DDM-grown *P. alexandrii* at different densities led to the formation of plaques on *T. pseudonana* soft-overlay plates. In contrast, ½YTSS-grown *P. alexandrii* yielded no (or few) plaques, even at equivalent bacterial densities (Fig. 3a). These experiments suggest that the capacity of *P. alexandrii* to cause plaque formation on *T. pseudonana* plates is induced by pregrowth on DDM.

To better characterise this phenomenon, we tested the impact of DDM vs ½YTSS-grown *P. alexandrii* on diatom growth in liquid culture. We inoculated diatom hosts into three different treatments: either growing them axenically or co-inoculating them with *P. alexandrii* pregrown on ½YTSS or DDM. Whereas growth of all five diatoms inoculated with *P. alexandrii* pregrown on ½YTSS was comparable to the axenic control, growth of *T. pseudonana*, *Skeletonema* sp. PLY627, and *Chaetoceros* sp. (PLY617) was completely impaired by DDM-grown *P. alexandrii* (Figs 3b,c, S4). Similarly, F_v/F_m of *T. pseudonana*, *Skeletonema* sp. PLY627, and *Chaetoceros* sp. PLY617 cells was undetectable when inoculated in co-culture with DDM-grown *P. alexandrii* cells (Day 8; Fig. 3d). Therefore, in concurrence with our plaque assay results, these data suggest that the growth inhibitory effect of *P. alexandrii* on diatoms is facultative, being activated only when cells are first grown on DDM. Moreover, we verified that *P. alexandrii* causes diatom cell death, using the live-dead stain SYTOX green. Inoculation of *T. pseudonana* with *P. alexandrii* not only led to reduced growth compared with axenic culture (Fig. S5A) but also 95% of cells detected were dead, indicating that this bacterium is algicidal (Fig. S5B). Moreover, epifluorescence microscopy revealed colonisation of *P. alexandrii* around single *T. pseudonana* cells after 48 h of co-culture inoculation (82% (28/34) of cells; Fig. S6), indicating that *P. alexandrii* can physically attach to *T. pseudonana* cells.

To further explore the sensitivity and thus environmental relevance of the conditional activation of *P. alexandrii* by pre-exposure to DDM, we grew *P. alexandrii* for 4 d on a serial dilution of *T. pseudonana* DDM from 1× (i.e. a 14-d-old culture of 3.3×10^6 cells ml^{-1}) down to a one-thousandth dilution (i.e. equivalent to 3300 cells ml^{-1}) and inoculated co-cultures with *T. pseudonana*. In all co-culture treatments with DDM-grown *P. alexandrii*, diatom growth was completely abolished after 7 d compared with the no bacteria (*P. a*) control (Fig. 4a). This was also the case for *P. alexandrii* pre-exposed to (1×) cell-free diatom filtrate. By contrast, ½YTSS-grown bacterial cells had no significant effect on *T. pseudonana* growth. Given the sensitivity of the activation of the growth inhibitory effect of *P. alexandrii* even to diluted DDM, we tested whether *P. alexandrii* inoculated into f/2 medium only (i.e. with no dead diatom matter) caused diatom growth inhibition. While *P. alexandrii* pregrown on f/2 medium did affect *T. pseudonana* after 4 d, by Day 7 there was only a 24% reduction in growth relative to the no bacteria control, compared with the 99% inhibitory effect of DDM-grown *P. alexandrii* at Day 7 (Fig. 4b). We also tested whether supplementation with liquid DDM at the point of co-culture inoculation activated the growth inhibitory effect of ½YTSS-grown *P. alexandrii* cells. This revealed statistically significant growth

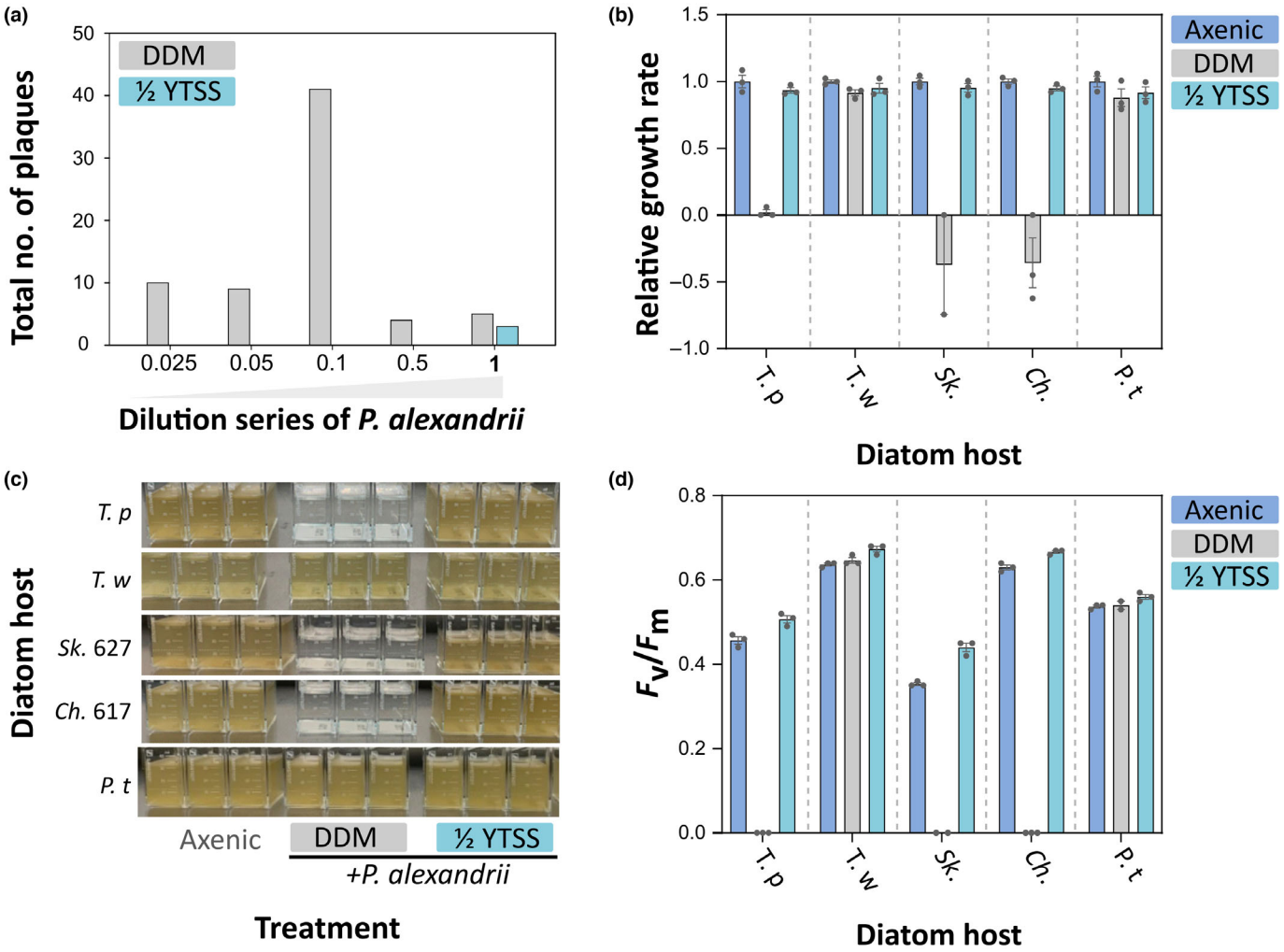

Fig. 3 *Ponticoccus alexandrii* inhibits diatom growth in a species-specific manner but only when pregrown on diatom organic matter. (a) Number of plaques when pure cultures of *P. alexandrii* were inoculated into plaque assays with *Thalassiosira pseudonana*, comparing different densities of bacteria. Before the plaque assay, *P. alexandrii* was grown either on agarose plates made up with autoclaved diatoms ('Dead Diatom Medium' (DDM)) or rich ½YTSS (Yeast Tryptone Sea Salts) medium. The 1× treatment represented a final OD600 of 0.01. (b) Growth rate relative to axenic control (measured during exponential growth phase) of all five diatom hosts *T. pseudonana* (*T. p*), *Thalassiosira weissflogii* (*T. w*), *Skeletonema* sp. PLY627 (*Sk.*), *Chaetoceros* sp. PLY617 (*Ch.*), and *Phaeodactylum tricornutum* (*P. t*) when inoculated with DDM- vs ½YTSS-grown *P. alexandrii*. Error bars indicate ±SEM for $n = 3$; individual data points are plotted. (c) Photographs of the cultures described in (b) on Day 9. (d) Maximum quantum efficiency of photosystem II (F_v/F_m) of cultures on Day 8. Error bars indicate ±SEM for $n = 3$; individual data points are plotted.

inhibition of *T. pseudonana* in the co-cultures when DDM was added directly into the liquid medium upon inoculation (that was not detected for co-cultures with ½YTTS grown bacteria without DDM amendment; Fig. 4c), albeit the effect was far less pronounced compared with experiments with *P. alexandrii* pregrown on DDM (Fig. 4a). Controls inoculating *T. pseudonana* with DDM but without *P. alexandrii* showed no growth inhibition at this time point, indicating that exposure of *T. pseudonana* to liquid DDM alone did not cause the observed negative impact on diatom growth. Finally, we examined the specificity of the conditional activation of *P. alexandrii* to diatom necromass vs media made up from other algal taxa. We pregrew *P. alexandrii* on dead media made up from either the coccolithophore *Isochrysis galbana* (*I. g*), or dinoflagellate *Amphidinium carterae* (*A. c*) and co-inoculated bacterial cells with *T. pseudonana*. Both treatments caused an almost complete reduction in *T. pseudonana* growth, comparable to that seen for *P. alexandrii* pregrown on *T. pseudonana* DDM (Fig. 4d). However, interestingly *P. alexandrii* did not exhibit any growth inhibitory effect against *A. carterae* (in any treatment) and caused a < 50% reduction in *I. galbana* growth when pregrown on either DDM or dead coccolithophore medium (Fig. 4d,e).

Activation of antagonistic activity by DDM is widespread amongst diverse WEC antagonists

We extended our approach to determine whether other WEC bacterial strains also exhibit growth inhibitory effects against diatoms, which are activated by pre-exposure to DDM. As we were primarily interested in antagonistic effects in planktonic

conditions, these experiments were conducted in liquid culture rather than via the plaque assay. We tested the impact of inoculating different bacterial isolates into co-culture with the diatom host from which they were originally isolated. We focussed these efforts predominantly on species for which there have been no prior reports of algicidal activity against diatoms. In total, we tested 11 bacterial species (including *P. alexandrii*), including *Thalassospira lohafexi*, *Vibrio diazotrophicus*, *Alteromonas simiduii*, *M. adhaerens*, *Halomonas titanicae*, *Metabacillus idriensis*, *Maribacter spongiicola*, *Marinobacter algicola*, *Pseudomonas lurida*, and

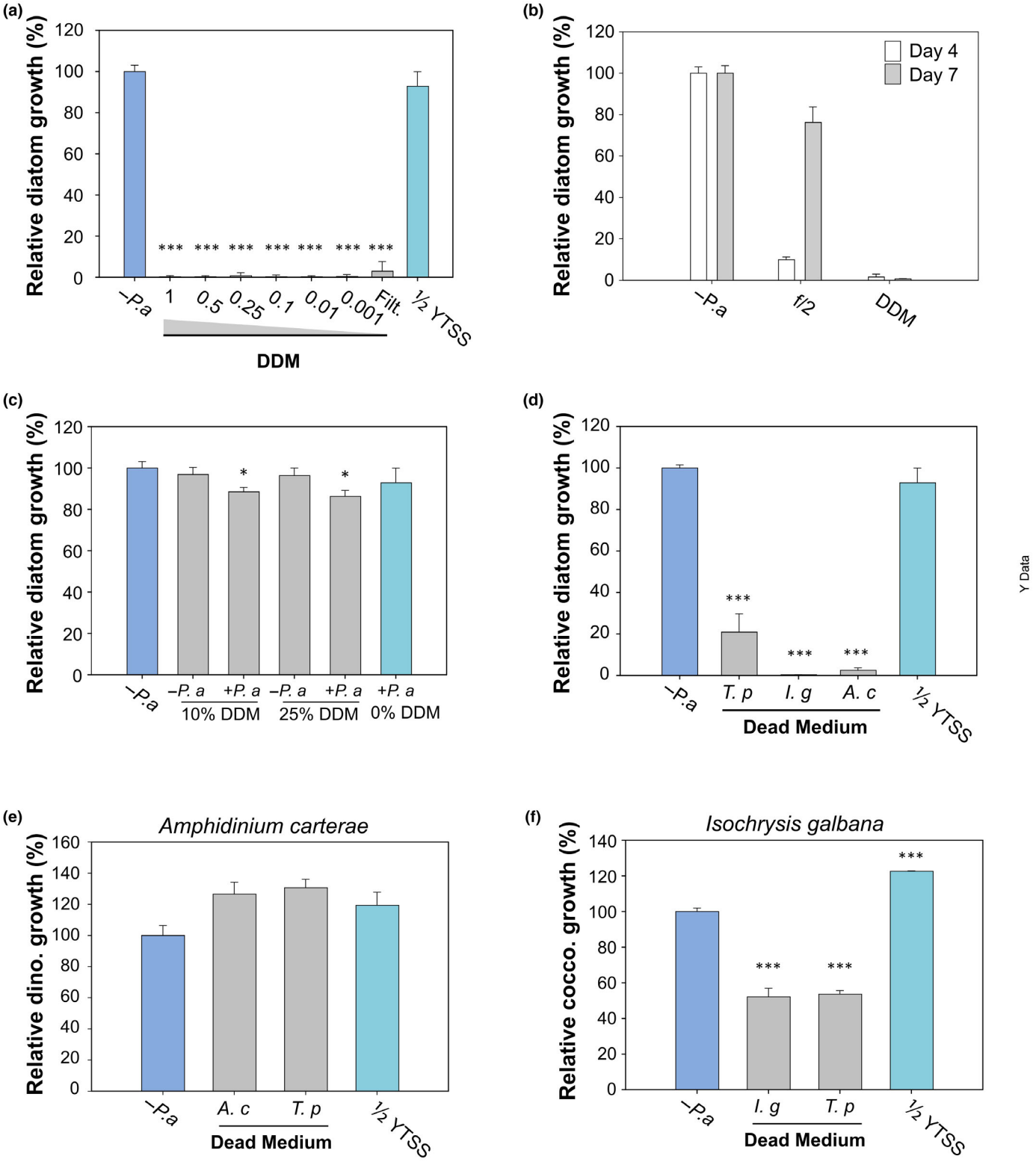

Fig. 4 Examining the sensitivity and specificity of the activation of algicidal behaviour of *Ponticoccus alexandrii* by algal necromass. (a) Percentage growth relative to the diatom-only control of *Thalassiosira pseudonana* inoculated into co-culture with *P. alexandrii ('P. a')* pregrown for 4 d on different dilutions of Dead Diatom Medium (DDM) from 1× (made from a 14-d-old culture at a cell density of 3.3×10^6 cells ml^{-1}) to a one-thousandth dilution (i.e. equivalent to 3300 cell ml^{-1}). The effect of *P. a* pre-grown on cell-free filtrate ('Filt') from the same 1 × *T. pseudonana* culture was also tested. A control treatment of ½YTSS (Yeast Tryptone Sea Salts) grown *P. alexandrii* inoculated to the same density (final optical density at 600 nm of 0.05) is also shown. (b) As shown in Part (a) but with *P. alexandrii* pregrown on f/2 only vs *T. pseudonana* DDM (on Days 4 and 7). (c) Percentage growth of *T. pseudonana* (relative to the standard *T. pseudonana* control without bacteria) grown in f/2 media supplemented with liquid DDM 10% or 25% (v/v) in the presence or absence of *P. alexandrii* ('*P. a*') pregrown for 4 d on ½YTSS. A control co-culture of *T. pseudonana* inoculated without DDM, that is '0% DDM' but with *P. alexandrii* pregrown on ½YTSS is also shown. (d) Percentage growth relative to the diatom-only control of *T. pseudonana* inoculated into co-culture with *P. alexandrii* ('*P. a*') pregrown for 4 d on dead media made up from *T. pseudonana* (*T. p*), the coccolithophore *Isochrysis galbana* (*I. g*) or dinoflagellate *Amphidinium carterae* (*A. c*). (e, f) Percentage growth relative to the algae only control of *A. carterae* (e) and *I. galbana* (f) inoculated into co-culture with *P. alexandrii ('P. a')* pregrown on autoclaved algal host medium, *T. pseudonana* DDM or ½YTSS. For all data shown in this figure, algal growth was quantified by measuring chlorophyll fluorescence after 7 d. Error bars indicate ±SEM for $n = 3$; *P*-values (one-way ANOVA comparing treatments to the algal monoculture control, dark blue): $*P < 0.05$; $***P < 0.001$ ($n = 3$).

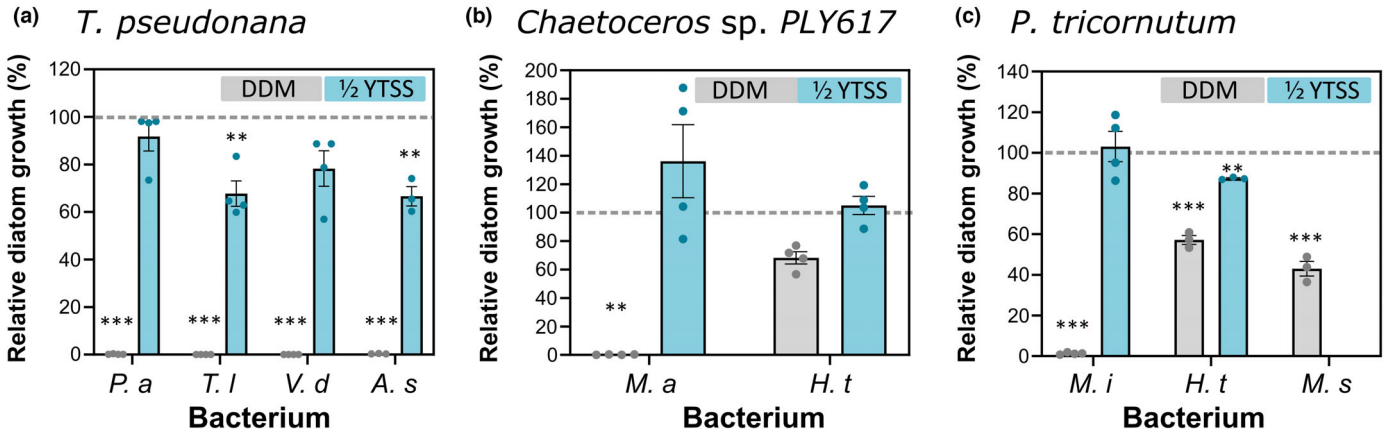

Fig. 5 Growth inhibitory effect against diatoms is activated by Dead Diatom Medium (DDM) in multiple other Western English Channel (WEC) plaque assay bacteria. Percentage growth relative to axenic control (marked by a dashed grey line) of the diatoms *Thalassiosira pseudonana* (a), *Chaetoceros* sp. PLY617 (b) and *Phaeodactylum tricornutum* (c) in the presence of WEC bacteria. Bacterial isolates tested included: *Ponticoccus alexandrii* (*P. a*), *Thalassospira lohafexi* (*T. l*), *Vibrio diazotrophicus* (*V. d*), and *Alteromonas simiduii* (*A. s*) for *T. pseudonana*; *Marinobacter adhaerens* (*M. a*), and *Halomonas titanicae* (*H. t*) for *Chaetoceros* sp. PLY617, as well as *Metabacillus idriensis* (*M. i*), *Halomonas titanicae* (*H. t*), and *Maribacter spongiicola* (*M. s*) for *P. tricornutum*. N. b. only *M. spongiicola* pregrown on DDM was tested. The effect on the growth of diatom host on which the bacterium was originally isolated was examined. Bacteria were inoculated to a final optical density at 600 nm of 0.05. Error bars indicate ±SEM for $n = 4$ or 3; individual data points are plotted. Growth was quantified by measuring diatom cell density (cells ml^{-1}) on 4–14 d (depending on the diatom host species) following inoculation into fresh f/2 media with or without WEC bacteria. *P*-values (one-way ANOVA comparing individual co-culture treatments to the axenic control): $P < 0.05$; **, $P < 0.01$; ***, $P < 0.001$ ($n = 3$ to 4). Individual data points are shown.

Oceanicaulis alexandrii. Inoculation of *T. pseudonana* with the *Alphaproteobacterium T. lohafexi* and *Gammaproteobacteria V. diazotrophicus* and *A. simiduii* pregrown on DDM caused an almost complete (99.8, 99.7, and 99.7%, respectively) decrease in diatom cell numbers relative to the axenic control (Fig. 5a; *P. alexandrii* was used as a positive control). By comparison, ½YTSS-grown *T. lohafexi*, *V. diazotrophicus*, and *A. simiduii* cells resulted in a decrease in *T. pseudonana* cell density by 32.3, 21.7, and 33.4%, respectively. Both *M. adhaerens* and *H. titanicae* also reduced growth of *Chaetoceros* sp. (PLY617; causing a 99.8 and 31.8% reduction in diatom density), but only when pregrown on DDM (Fig. 5b). We also verified the antagonistic effect against *P. tricornutum* of *M. idriensis*, *H. titanicae*, and *M. spongiicola* that caused a 98.7, 42.8, and 67.7% reduction in diatom cell numbers when pregrown on DDM, respectively, compared with the diatom-only control (Fig. 5c).

However, not all the bacteria isolated via our plaque assay approach could be verified to affect diatom growth in liquid culture. Inoculating *M. algicola* into co-culture with *Skeletonema* sp. PLY627 or *T. weissflogii* did not cause significant reductions in diatom growth in any treatment examined (Fig. S7), even though 'plaque-to-plaque' assays inoculating from *M. algicola* plaques did lead to the formation of multiple new plaques on *T. pseudonana* (Table S2). For *P. lurida*, we observed an 11.7 and 21.3% inhibition of diatom host growth (when pregrown on DDM or ½YTSS, respectively) relative to the axenic control (Fig. S7). Similarly, ½YTSS-grown *O. alexandrii* caused a 20.8% reduction in *T. weissflogii* growth, but this was not significant. Thus, under the conditions examined, we have not been able to conclusively verify that these bacteria are diatom antagonists. However, we have verified that eight of the 11 bacterial isolates tested do confer robust growth inhibitory effects against diatoms (Fig. 5).

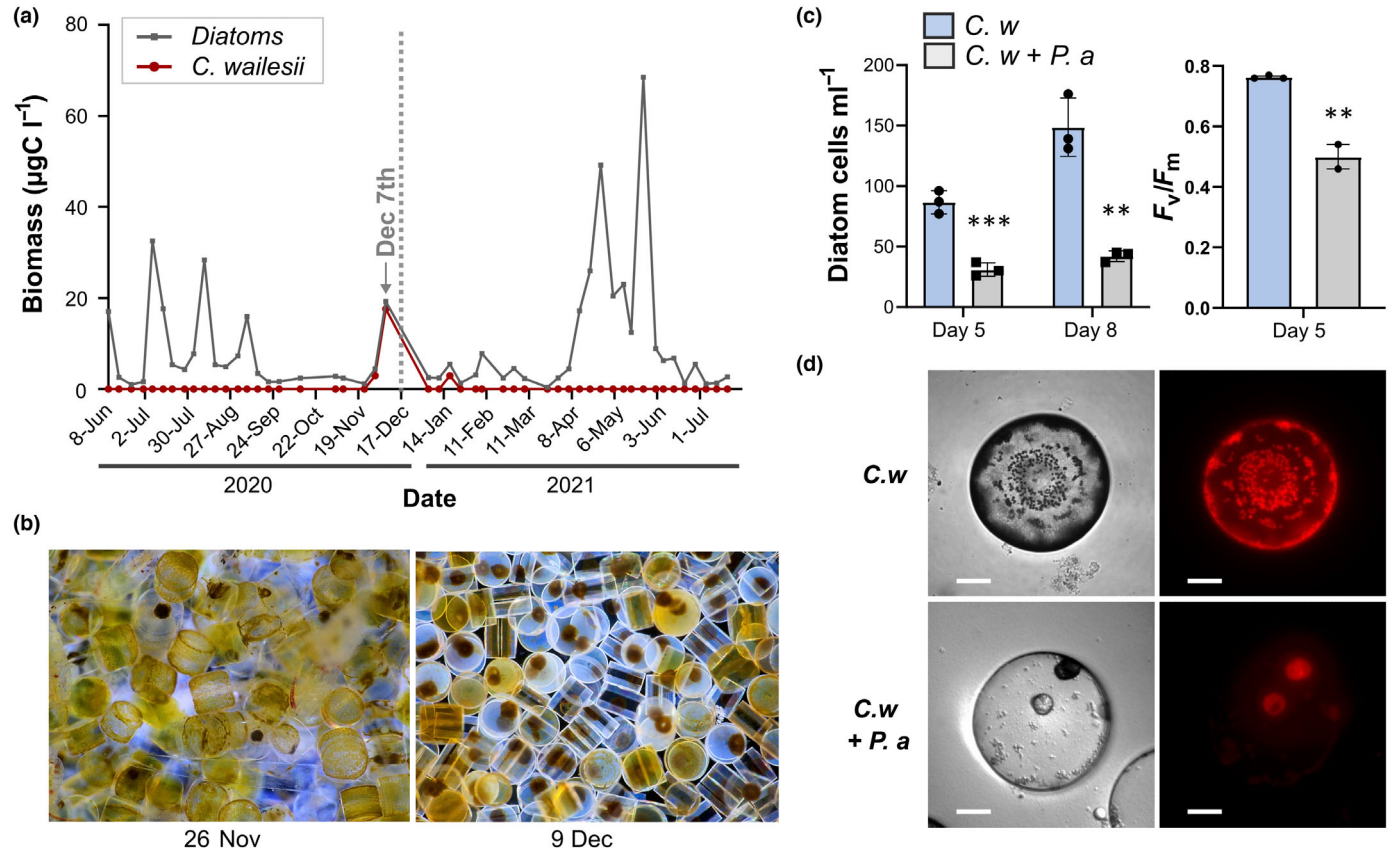

Fig. 6 Peaks in plaque enumeration corresponded with senescence of a winter diatom bloom. (a) Total biomass (µgC l^{-1}) of diatoms making up a winter diatom bloom at L4 station in late 2020. The centric diatom *Coscinodiscus wailesii* accounted for the majority of biomass during this bloom. Data were collected by the Western Channel Observatory (WCO) (https://www.westernchannelobservatory.org.uk/). The December plaque assay sampling date (17 December 2020) is indicated with a dashed grey line. The WCO sampling date (7 December) just before this is also highlighted (grey arrow). The WCO sampling point after this was 4 January. (b) Light microscopy images of *Coscinodiscus wailesii* cells sampled from L4 on 26 November and 9 December (©Richard Kirby). The diameter of *Coscinodiscus* is *c*. 350 µm. (c) Impact *of Ponticoccus alexandrii* on *C. wailesii* growth and F_v/F_m after 5 and 8 d. On Day 8, F_v/F_m values for *C. wailesii* + *P. alexandrii* were undetectable vs 0.55 ± 0.01 in the control. *P*-values (Student's *t*-test): **, $P < 0.01$; ***, $P < 0.001$ ($n = 3$). (d) Bright-field images (left) of example *C. wailesii* cells 6-d postinoculation with or without *P. alexandrii*. Bacteria were inoculated to a final optical density at 600 nm of 0.05. Epifluorescence images of chlorophyll autofluorescence are also shown (Left). Bar, 50 µm.

Peaks in antagonistic activity in the WEC coincided with senescence of a winter diatom bloom

Having verified that the plaque assay sampling approach has successfully isolated antagonistic bacteria capable of inhibiting diatom growth, we investigated broader ecosystem trends relating to patterns in plaque enumeration over our sampling. Of particular note was the large peak in plaques recorded in December 2020 (Fig. 1c). Environmental metadata indicated relatively high nutrient concentrations, low light and sea temperatures during this period, as is typical of the winter months at L4 station (Fig. S8). Examination of diatom diversity and abundance data collected via the WCO revealed that a winter diatom bloom was in progress in December 2020 (Fig. 6a). The centric diatom *Coscinodiscus wailesii* accounted for *c*. 92% of diatom biomass at the peak of this bloom (on 7 December), with diatoms making up 83.9% of the total phytoplankton biomass. *Thalassiosira* but not *Skeletonema* and *Chaetoceros* were also present (Fig. S9A,B). Notably, images of phytoplankton taken during the bloom revealed that by 9 December *Coscinodiscus* cells were senescing with chloroplastic material coalescing within the cell, compared with earlier images taken on 26 November where chloroplastic material was generally intact (Fig. 6b). This was 8 d before our plaque assay sampling date (17 December). As the peak in plaque enumeration did not occur with peaks in total abundance of heterotrophic bacteria during our 13-month sampling window (Fig. S9C), we conclude that the substantially higher number of plaques detected in December 2020 was due to an increased contribution of bacterial antagonists to total bacterial abundance. As one of the bacteria detected during this bloom was *P. alexandrii* (Fig. 2d), we tested whether C. *wailesii* is susceptible to *P. alexandrii*. We isolated a local WEC strain of *C. wailesii* (the 'Materials and Methods' section), Inoculation into co-culture with *P. alexandrii* caused a substantial reduction in growth and F_v/F_m of this strain compared with the no *P. alexandrii* control (Fig. 6c). Moreover, cells looked less healthy with empty frustules often observed (Fig. 6d). Together, our evidence indicates that antagonistic bacteria showing increased abundance during senescence of a bloom of *C. wailesii* are capable of robust growth inhibitory effects against this diatom.

Global biogeography of WEC bacterial isolates and their co-occurrence with diatom hosts

To determine the broader biogeography of WEC antagonists, we searched for their distribution in marine ecosystems globally analysing the Ocean Barcode Atlas (Karsenti *et al.*, 2011; Vernette *et al.*, 2021). We queried the *Tara* Oceans 16S/18S miTAG metabarcode database with representative 16S rRNA gene sequences of our WEC isolates (Dataset S2). The resemblance of 16S rRNA gene query sequences of WEC isolates was assessed by compiling maximum likelihood trees for each taxon (Methods S1; Figs S10–S13). Using this approach, we detected metabarcodes for *T. lohafexi* (or its close relative *T. lucentensis*; Shivaji *et al.*, 2015), *M. adhaerens*, and *H. titanicae* (Table S3). While we also identified putative hits for *P. alexandrii* and *M. idriensis*, reads were not detected in the SRF or DCM samples. Additionally, we could not identify close homologues for *M. spongiicola* nor *V. diazotrophicus*. However, we could identify a hit for *M. dokdonensis* (Fig. S11) that is closely related to *Maribacter* sp. PML-EC2, an algicidal bacterium previously isolated from the WEC that inhibits the growth of *Skeletonema* sp. (Wang *et al.*, 2016; Fig. S11). We therefore examined the distribution of *M. dokdonensis* too. In total, metabarcodes of these four bacterial species were detected in 29 different stations, spanning 7 ocean regions including the S. Pacific, N. Pacific, Mediterranean Sea, Red Sea, Indian Ocean, S. Atlantic, and Arctic Oceans (Fig. S14; Table S4). *H. titanicae* was the most widespread, identified at 13 *Tara* stations, compared with *T. lohafexi* (12 stations), *M. dokdonensis* (9 stations), and *M. adhaerens* (8 stations). We detected a particularly high incidence of these bacteria in the Mediterranean Sea, with all four represented at station Tara_009, and three of the four (*T. lohafexi*, *M. dokdonensis*, and *M. adhaerens*) detected at TARA_007.

To investigate whether we could detect co-occurrence of bacteria with diatom hosts, we also examined the distribution of *T. pseudonana*, *Skeletonema* sp., and *Chaetoceros* sp. that exhibit susceptibility to at least one of these bacteria (Fig. 5; Wang *et al.*, 2016). This analysis revealed co-occurrence of *T. pseudonana* metabarcodes (Table S5; the 'Materials and Methods' section) with *T. lohafexi* at stations in the Mediterranean Sea and Arctic Ocean (Fig. 7a). Likewise, we observed co-occurrence of *Skeletonema* sp. metabarcodes (Fig. S15) at six stations with *M. dokdonensis*, including in the South Atlantic and Mediterranean Sea (Fig. 7b). Finally, *Chaetoceros* sp., (Fig. S16) showed overlapping biogeography with both *M. adhaerens* and *H. titanicae* in the Mediterranean Sea, South Pacific, Red Sea, and Indian Ocean (Fig. 7c). In conclusion, we report the widespread distribution of several WEC isolates and show their co-occurrence with diatom hosts in different ocean regions, for several interactions validated in the laboratory.

Discussion

Despite accumulating evidence that bacterial pathogens can profoundly impact the growth and physiology of diatoms (Amin *et al.*, 2012; Van Tol *et al.*, 2017), their prevalence and dynamics in natural marine ecosystems are poorly understood. To address this fundamental knowledge gap, we have conducted a 13-month sampling effort to systematically characterise the diversity and seasonal patterns of diatom antagonistic bacteria in a productive coastal ecosystem, where diatoms frequently bloom. We report that multiple and diverse bacterial antagonists co-occur with bloom-forming diatoms in this region. The identification of numerous bacterial species that had no prior reports of antagonistic activity towards diatoms, coupled with our observation that this activity was evident only when antagonists were pre-exposed to diatom organic matter, indicates that bacterial pathogenicity towards diatoms is more prevalent than previously recognised. Moreover, our study captures important evidence of increased detection of bacterial antagonists during senescence of a diatom bloom. We subsequently isolated the major diatom dominating the bloom, *C. wailesii*, and confirmed its susceptibility to *P. alexandrii* that was identified in multiple plaques obtained during this bloom. *C. wailesii* in co-culture with *P. alexandrii* exhibited similar 'symptoms' to those observed in *in situ Coscinodiscus* cells visualised just before our sampling point that detected increased plaque numbers. Finally, we identified that many of the WEC antagonists identified in this study exhibit geographical ranges extending beyond the WEC and co-occur with diatom hosts in regions ranging from the Mediterranean Sea to the Arctic Ocean. Our work raises important questions regarding the influences of diatom pathogens on natural diatom populations at the global scale.

The plaque assay approach has successfully enabled isolation of bacterial antagonists from clearance plaques on semisolid diatom lawns. This environment is considerably different from that of planktonic diatoms living in the ocean, with diatom cells significantly more concentrated, immobilised, and likely experiencing high nutrient and cellular stress in diatom lawns. Despite this, we observed substantial growth inhibitory effects of multiple bacteria isolated from plaque assays in liquid culture. The highly sensitive conditional activation of algicidal behaviour by diluted DDM of the recurrent isolate *P. alexandrii*, alongside its ability to colonise diatom cells in liquid culture further highlights the environmental relevance of our system to planktonic communities. The modest inhibitory effect of f/2-grown *P. alexandrii* on *T. pseudonana* growth suggests that nutrient starvation may be a component of this conditional activation. However, as DDM-grown *P. alexandrii* had the most pronounced and prolonged effect on diatoms, detection of algal metabolites clearly exacerbates the algicidal activity of *P. alexandrii*. It is also important to note that not all plaque assay isolates showed growth inhibitory effects. This could be because on certain occasions the plaque assay isolated more than one bacterium from a single plaque (e.g. *M. algicola*, which did not show growth inhibitory effects against diatoms under the conditions tested). However, as the other bacterium (*Aestuarilvita* sp.) co-isolated with *M. algicola* could not be maintained following isolation, its effects on diatom growth could not be tested. The potential of a plaque to contain more than one bacterium highlights the need for physiological characterisation of pure isolates following isolation to verify growth inhibitory effects of putative antagonists. Indeed, we were able to confirm robust

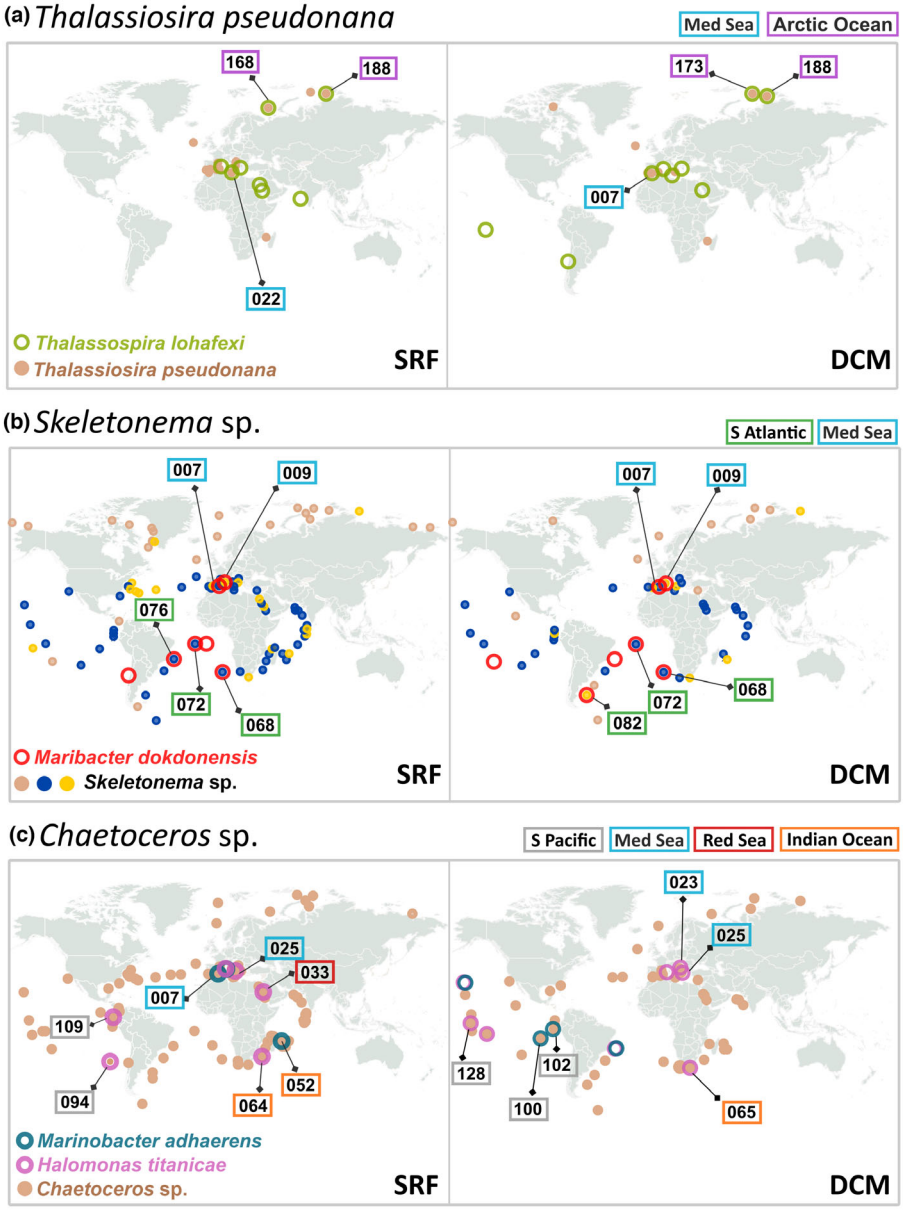

Fig. 7 Global biogeography of WEC bacterial isolates with verified antagonistic activity towards diatoms and their co-occurrence with diatom host taxa. (a) Global distributions of *Thalassospira lohafexi* and *Thalassiosira pseudonana* metabarcode hits in the surface (SRF) waters and Deep Chlorophyll Maxima (DCM), as determined through searching the *Tara* Ocean Barcode Atlas (Vernette *et al*., 2021). TARA stations where co-occurrence of diatom host and bacteria metabarcodes are detected are labelled on the figure. (b) Distributions of *Maribacter dokdonensis* and *Skeletonema* sp. metabarcode hits are shown, labelled as described in Part (a). For *Skeletonema* sp., hits are colour coded according to phylogeny: Brown indicates where only metabarcodes resembling *Skeletonema marinoi* were found, yellow shows locations where both *S. marinoi*-like and *Skeletonema menzelii*-like sequences were observed, and blue indicates locations where only *S. menzelii*-like sequences were represented (Fig. S15). (c) Distributions of *Marinobacter adhaerens* and *Chaetoceros* sp. metabarcode hits are shown, labelled as described in Part (a).

growth inhibitory effects against diatoms of 8 of 11 bacterial isolates tested.

Whereas the vast majority of studies of natural diatom populations typically focus on spring in order to capture spring phytoplankton blooms, our study highlights the importance of monitoring the full seasonal cycle. Winter and autumnal diatom blooms are not uncommon, with phytoplankton populations often having a distinct community composition during these seasons (Widdicombe *et al*., 2010). In the WEC, the centric diatoms *Coscinodiscus* spp. and *Odontella mobiliensis*, as well as the benthic diatoms *Paralia sulcate* and *Podosira stelligera*, dominate winter communities (Widdicombe *et al*., 2010). Nanodiatoms including *Minidiscus comicus* and *T. profunda* also peak principally during winter (Arsenieff *et al*., 2020). Despite being a key component of WEC phytoplankton communities (Arsenieff *et al*., 2020) and global carbon export (Leblanc *et al*., 2018), these tiny diatoms are typically overlooked in routine monitoring due to challenges in their identification. Our observation of peak plaque detection during winter but not spring suggests that antagonistic bacterial populations may co-occur with, and exert influence on, specific diatom host populations. Whether the peak in plaque abundance observed reflects increases in the antagonist abundance, algicidal activity, or a combination of both, remains an open question. However, these important observations provide new opportunities to further dissect the dynamics of antagonistic diatom–bacteria interactions that may be key drivers of diatom blooms and population health in marine ecosystems. This is particularly important in the light of evidence that *C. wailesii* (formerly *C. nobilis* Grunow; Gomez & Souissi, 2010) can have severe detrimental impacts on coastal ecosystems, with extensive mucus production causing clogging of fishing nets in the WEC (Boalch & Harbour, 1977).

The taxonomic composition of our library of WEC antagonistic bacteria was made up predominantly of *Alphaproteobacteria* (44% of species isolated), followed by *Gammaproteobacteria* (39%), *Flavobacteria* (11%), and finally members of the *Bacilli* (0.06%). This contrasts with literature evidence from over 100 published papers, which showed that the majority of diatom algicidal bacteria belong to the *Gammaproteobacteria* (42%), compared to just 0.08% representing the *Alphaproteobacteria* (Coyne *et al.*, 2022). However, this encompasses bacteria isolated from a variety of sources. As many reports focussed on a single bacterial isolate from their sample/environment, these data likely do not reflect the true make-up of antagonist populations in any one marine ecosystem. By sampling frequently and over an annual cycle in the WEC, we have gained a greater sampling depth. Our study also addresses a clear bias in sampling efforts towards the study of algicidal bacteria of dinoflagellates (with 116 bacterial species reported), compared to those of diatoms (38 bacterial species; Coyne *et al.*, 2022). Nevertheless, our study may too have been affected by inherent sampling biases. Specific bacterial taxa (e.g. culturable vs unculturable species) are likely more amenable to plaque assay isolation than others. A conspicuous absence of several of the 'usual suspects' was also apparent. We did not detect any *Croceibacter* (Van Tol *et al.*, 2017) or *Cytophaga*, and only one *Alteromonas* and one *Vibrio* species were isolated, despite these taxa being frequently reported as algicidal (Mayali & Azam, 2004). It is possible that these bacteria are more representative of oceanic systems (Van Tol *et al.*, 2017) or the distinct geographic regions (Mitsutani *et al.*, 1992; Imai *et al.*, 1993) from which they were isolated. Certainly, our isolation of *P. alexandrii* on 19 independent occasions from the WEC, despite only one prior report of this species being algicidal (Chi *et al.*, 2017), suggests it may be particularly prevalent in coastal WEC waters.

The predominance of *Alphaproteobacteria* amongst our library of WEC antagonists challenges current perceptions of the 'good' vs 'bad' members of the diatom microbiome. *Alphaproteobacteria* are frequently observed to facilitate diatom growth through provision of nutrients or exerting a protective effect (Hünken *et al.*, 2008; Amin *et al.*, 2015; Durham *et al.*, 2015; Suleiman *et al.*, 2016). Similarly, we observed a robust growth inhibitory effect of *M. adhaerens* against *Chaetoceros* sp. PLY617, despite this bacterium more commonly being considered a diatom commensal (Gärdes *et al.*, 2012; albeit a subtle inhibitory effect on *Coscinodiscus radiatus* growth by this bacterium was recently reported; Deng *et al.*, 2022). Indeed, this effect was only observed when cells were first grown on medium made up of autoclaved diatoms. By comparison, *M. adhaerens* pregrown on ½YTSS medium appeared to stimulate diatom growth. This concept of a 'sliding scale' from synergistic to antagonistic is not new in marine microbial ecology. Jekyll-and-Hyde dynamics towards coccolithophores have also been observed for *Rhodobacteraceae* bacteria *Phaeobacter* (Seyedsayamdost *et al.*, 2011) and *Sulfitobacter* (Barak-Gavish *et al.*, 2018, 2023). However, our evidence suggests this 'switch' towards antagonistic behaviour may be more common than previously recognised, with the growth inhibitory effects of bacterial species spanning seven different bacterial orders tested being enhanced by pregrowth on DDM. However, we also observed differences in the dynamics of our system. Whereas *Sulfitobacter* D7 pregrown on ½YTSS 'coexisted' with the coccolithophore *Emiliania huxleyi* for *c.* 7 d before becoming pathogenic (Barak-Gavish *et al.*, 2023), ½YTSS-grown *P. alexandrii* did not cause a culture crash of susceptible diatoms even after 16 d. In the *E. huxleyi*-*Sulfitobacter* system, the signalling molecule algal-derived dimethylsulfoniopropionate (DMSP) was identified to be pivotal for mediating the transition to pathogenicity, whereas benzoate hindered this switch (Barak-Gavish *et al.*, 2023). Whether bacterial antagonists perceive different cues depending on the algal host remains an open question, particularly as diatoms are typically considered 'low DMSP producers' compared with coccolithophores (McParland & Levine, 2019). However, our evidence that dead coccolithophore (*I. galbana*) and dinoflagellate (*A. carterae*) medium also activate the algicidal behaviour of *P. alexandrii* (against *T. pseudonana*) suggests certain cues may be common between algal taxa. Albeit *P. alexandrii* showed reduced or no growth inhibitory effects towards these algae, respectively. This is despite previous reports of another strain (*Ponticoccus* sp. PD-2) being algicidal towards dinoflagellates. A key open question remaining is the mechanism by which *P. alexandrii* and other WEC isolates confer growth inhibitory effects. The algicidal compounds released by *Phaeobacter* species (roseobacticides; Seyedsayamdost *et al.*, 2011) are not synthesised by all *Roseobacter* species (Sonnenschein *et al.*, 2018), and algicidal mechanisms are multifaceted (Meyer *et al.*, 2017). The isolation of multiple, diverse bacterial antagonists co-occurring in the WEC offers exciting new opportunities to examine the evolution and ecology of pathogenic strategies amongst bacteria occupying the same niche.

Alpha- and *Gammaproteobacteria* (as well as *Flavobacteria*) are often reported to be associated with diatoms and diatom blooms. Indeed, accumulating evidence suggests that representatives of these groups are specialised for decomposition of algal-derived organic matter (Teeling *et al.*, 2012), and certain species including *M. adhaerens* physically interact with diatom aggregates (Gärdes *et al.*, 2010; Kaeppel *et al.*, 2012). However, the roles of algicidal bacteria in controlling natural diatom blooms are not well understood. Mesocosm experiments inoculating the algicidal bacterium *K. algicida* into plankton samples taken during a North Sea diatom bloom caused rapid decline of *Chaetoceros* populations (Bigalke *et al.*, 2019). However, whether bacterial populations reach sufficient densities in nature to confer such an effect remains an open question. This is particularly pertinent given that density-dependent quorum sensing has been shown to regulate growth inhibitory effects of *Ponticoccus* sp. *PD-2* against the dinoflagellate *Prorocentrum donghaiense* (Chi *et al.*, 2017). Intriguingly, we observed peaks in plaque detection that co-occurred with senescence of a winter diatom bloom. As total levels of heterotrophic bacteria did not reach peak abundance at the same time, our data suggest enrichment of antagonistic bacteria and/or their activity during this bloom. Further work is now required to determine whether such taxa contribute to diatom bloom demise or are opportunistically scavenging on decaying organic matter as a bloom wanes. Reports of declining diatom populations in the WEC (Widdicombe *et al.*, 2010) must also be considered in the light of our findings that multiple and persistent diatom antagonists inhabit this region.

Acknowledgements

We acknowledge support from the NERC Independent Research Fellowship grant NE/R015449/2 (KEH) and PhD studentship from the NERC ARIES doctoral training programme NE/S007334/1 (LB). CEW was supported by funding from the NERC National Capability Long-term Single Centre Science Programme, Climate Linked Atlantic Sector Science, grant no. NE/R015953/1. We also thank the crew of the research vessel Sepia (MBA, Plymouth, UK) for their collection of samples used during this study.

Competing interests

None declared.

Author contributions

KEH, LB, WW and MC planned and designed the research. LB, EH, CZYD, CS and CW performed experiments and analysed data. MK isolated strains underpinning the research. KH, LB, MC, CW and WW interpreted data and wrote the manuscript.

ORCID

Michael Cunliffe https://orcid.org/0000-0002-6716-3555
Ellen L. Harrison https://orcid.org/0000-0003-2592-8377
Katherine Helliwell https://orcid.org/0000-0002-2068-576X
Matthew Keys https://orcid.org/0009-0004-7609-3407
Courtney Swink https://orcid.org/0000-0002-3590-5040
Claire Widdicombe https://orcid.org/0000-0002-1688-0212

Data availability

Sequence data of bacterial strains isolated during this study are deposited in NCBI GenBank with accession nos.: OR776937–OR776933.

References

Aiyar P, Schaeme D, García-Altares M, Flores DC, Dathe H, Hertweck C, Sasso S, Mittag M. 2017. Antagonistic bacteria disrupt calcium homeostasis and immobilize algal cells. *Nature Communications* **8**: 1756.

Amin SA, Hmelo LR, Van Tol HM, Durham BP, Carlson LT, Heal KR, Morales RL, Berthiaume CT, Parker MS, Djunaedi B *et al.* 2015. Interaction and signalling between a cosmopolitan phytoplankton and associated bacteria. *Nature* **522**: 98–101.

Amin SA, Parker MS, Armbrust EV. 2012. Interactions between diatoms and bacteria. *Microbiology and Molecular Biology Reviews* **76**: 667–684.

Armbrust EV. 2009. The life of diatoms in the world's oceans. *Nature* **459**: 185–192.

Arsenieff L, Le Gall F, Rigaut-Jalabert F, Mahé F, Sarno D, Gouhier L, Baudoux AC, Simon N. 2020. Diversity and dynamics of relevant nanoplanktonic diatoms in the Western English Channel. *The ISME Journal* **14**: 1966–1981.

Barak-Gavish N, Dassa B, Kuhlisch C, Nussbaum I, Brandis A, Rosenberg G, Avraham R, Vardi A. 2023. Bacterial lifestyle switch in response to algal metabolites. *eLife* **12**: e84400.

Barak-Gavish N, Frada MJ, Ku C, Lee PA, DiTullio GR, Malitsky S, Aharoni A, Green SJ, Rotkopf R, Kartvelishvily E *et al.* 2018. Bacterial virulence against an oceanic bloom-forming phytoplankter is mediated by algal DMSP. *Science Advances* **4**: eaau5716.

Bartolek Z, Creveld SG, Coesel S, Cain KR, Schatz M, Morales R, Armbrust E. 2022. Flavobacterial exudates disrupt cell cycle progression and metabolism of the diatom *Thalassiosira pseudonana*. *ISME Journal* **16**: 1–11.

Bigalke A, Meyer N, Papanikolopoulou LA, Wiltshire KH, Pohnert G. 2019. The algicidal bacterium *Kordia algicida* shapes a natural plankton community. *Applied and Environmental Microbiology* **85**: e02779-18.

Boalch GT, Harbour DS. 1977. Unusual diatom off the coast of south-west England and its effect on fishing. *Nature* **269**: 687–688.

Buchan A, LeCleir GR, Gulvik CA, Gonzalez JM. 2014. Master recyclers: features and functions of bacteria associated with phytoplankton blooms. *Nature Reviews Microbiology* **12**: 686–698.

Chi W, Zheng L, He C, Han B, Zheng M, Gao W, Sun C, Zhou G, Gao X. 2017. Quorum sensing of microalgae associated marine *Ponticoccus* sp. PD-2 and its algicidal function regulation. *AMB Express* **7**: 1–10.

Cole JJ, Findlay S, Pace ML. 1988. Bacterial production in fresh and saltwater ecosystems: a cross-system overview. *Marine Ecology Progress Series* **43**: 1–10.

Coyne KJ, Wang Y, Johnson G. 2022. Algicidal bacteria: a review of current knowledge and applications to control harmful algal blooms. *Frontiers in Microbiology* **13**: 1–23.

Deng Y, Mauri M, Vallet M, Staudinger M, Allen RJ, Pohnert G. 2022. Dynamic diatom-bacteria consortia in synthetic plankton communities. *Applied and Environmental Microbiology* **88**: e0161922.

Ducklow HW, Kirchman DL, Quinby HL, Carlson CA, Dam HG. 1993. Stocks and dynamics of bacterioplankton carbon during the spring bloom in the eastern North Atlantic Ocean. *Deep Sea Research Part II: Topical Studies in Oceanography* **40**: 245–263.

Dungca-Santos JCR, Caspe FJO, Tablizo FA, Purganan DJE, Azanza RV, Onda DFL. 2019. Algicidal potential of cultivable bacteria from pelagic waters against the toxic dinoflagellate *Pyrodinium bahamense* (Dinophyceae). *Journal of Applied Phycology* **31**: 3721–3735.

Durham BP, Sharma S, Luo H, Smith CB, Amin SA, Bender SJ, Dearth SP, Van Mooy BAS, Campagna SR, Kujawinski EB *et al.* 2015. Cryptic carbon and sulfur cycling between surface ocean plankton. *Proceedings of the National Academy of Sciences, USA* **112**: 453–457.

Gärdes A, Iversen MH, Grossart HP, Passow U, Ullrich MS. 2010. Diatom-associated bacteria are required for aggregation of *Thalassiosira weissflogii*. *The ISME Journal* **5**: 436–445.

Gärdes A, Ramaye Y, Grossart HP, Passow U, Ullrich MS. 2012. Effects of *Marinobacter adhaerens* HP15 on polymer exudation by *Thalassiosira weissflogii* at different N : P ratios. *Marine Ecology Progress Series* **461**: 1–14.

Gilbert JA, Field D, Swift P, Newbold L, Oliver A, Smyth T, Somerfield PJ, Huse S, Joint I. 2009. The seasonal structure of microbial communities in the Western English Channel. *Environmental Microbiology* **11**: 3132–3139.

Gilbert JA, Steele JA, Caporaso JG, Steinbrück L, Reeder J, Temperton B, Huse S, McHardy AC, Knight R, Joint I *et al.* 2012. Defining seasonal marine microbial community dynamics. *ISME Journal* **6**: 298–308.

Gomez F, Souissi S. 2010. The diatoms *Odontella sinensis*, *Coscinodiscus wailesii* and *Thalassiosira punctigera* in the European Atlantic: recent introductions or overlooked in the past. *Fresenius Environmental Bulletin* **19**: 1424–1433.

Grossart H-P, Levold F, Allgaier M, Simon M, Brinkhoff T. 2005. Marine diatom species harbour distinct bacterial communities. *Environmental Microbiology* **7**: 860–873.

Guillard RRL, Ryther JH. 1962. Studies of marine planktonic diatoms. I. *Cyclotella nana* Hustedt, and *Detonula confervacea* (cleve) Gran. *Canadian Journal of Microbiology* **8**: 229–239.

Han MS, Furuya K. 2000. Size and species-specific primary productivity and community structure of phytoplankton in Tokyo Bay. *Journal of Plankton Research* **22**: 1221–1235.

Helliwell KE, Shibl AA, Amin SA. 2022. The diatom microbiome: new perspectives for diatom-bacteria symbioses. *The Molecular Life of Diatoms* **9**: 679–712.

Hünken M, Harder J, Kirst GO. 2008. Epiphytic bacteria on the Antarctic ice diatom *Amphiprora kufferathii* Manguin cleave hydrogen peroxide produced during algal photosynthesis. *Plant Biology (Stuttgart, Germany)* **10**: 519–526.

Imai I, Ishida Y, Hata Y. 1993. Killing of marine phytoplankton by a gliding bacterium *Cytophaga* sp., isolated from the coastal sea of Japan. *Marine Biology: International Journal on Life in Oceans and Coastal Waters* **116**: 527–532.

Jiao N, Herndl GJ, Hansell DA, Benner R, Kattner G, Wilhelm SW, Kirchman DL, Weinbauer MG, Luo T, Chen F *et al.* 2010. Microbial production of recalcitrant dissolved organic matter: long-term carbon storage in the global ocean. *Nature Reviews. Microbiology* **8**: 593–599.

Kaeppel EC, Gärdes A, Seebah S, Grossart HP, Ullrich MS. 2012. *Marinobacter adhaerens* sp. nov., isolated from marine aggregates formed with the diatom *Thalassiosira weissflogii*. *International Journal of Systematic and Evolutionary Microbiology* **62**: 124–128.

Karsenti E, Acinas SG, Bork P, Bowler C, de Vargas C, Raes J, Sullivan M, Arendt D, Benzoni F, Claverie JM *et al.* 2011. A holistic approach to marine eco-systems biology. *PLoS Biology* **9**: e1001177.

Kim J, Lyu XM, Lee JJL, Zhao G, Chin SF, Yang L, Chen WN. 2018. Metabolomics analysis of *Pseudomonas chlororaphis* JK12 algicidal activity under aerobic and micro-aerobic culture condition. *AMB Express* **8**: 131.

Lane DJ, Pace B, Olsen GJ, Stahl DA, Sogin ML, Pace NR. 1985. Rapid determination of 16S ribosomal RNA sequences for phylogenetic analyses. *Proceedings of the National Academy of Sciences, USA* **82**: 6955–6959.

Laundon D, Mock T, Wheeler G, Cunliffe M. 2021. Healthy herds in the phytoplankton: the benefit of selective parasitism. *ISME Journal* **15**: 2163–2166.

Leblanc K, Quéguiner B, Diaz F, Cornet V, Michel-Rodriguez M, Durrieu de Madron X, Bowler C, Malviya S, Thyssen M, Grégori G *et al.* 2018. Nanoplanktonic diatoms are globally overlooked but play a role in spring blooms and carbon export. *Nature Communications* **9**: 953.

Li D, Zhang H, Fu L, An X, Zhang B, Li Y, Chen Z, Zheng W, Yi L, Zheng T. 2014. A novel algicide: evidence of the effect of a fatty acid compound from the marine bacterium, *Vibrio* sp. BS02 on the harmful dinoflagellate, *Alexandrium tamarense*. *PLoS ONE* **9**: e91201.

Lu X, Zhou B, Xu L, Liu L, Wang G, Liu X, Tang X. 2016. A marine algicidal Thalassospira and its active substance against the harmful algal bloom species *Karenia mikimotoi*. *Applied Microbiology and Biotechnology* **100**: 5131–5139.

Malviya S, Scalco E, Audic S, Vincent F, Veluchamy A, Poulain J, Wincker P, Iudicone D, de Vargas C, Bittner L *et al.* 2016. Insights into global diatom distribution and diversity in the world's ocean. *Proceedings of the National Academy of Sciences, USA* **113**: E1516–E1525.

Mayali X, Azam F. 2004. Algicidal bacteria in the sea and their impact on algal blooms. *Journal of Eukaryotic Microbiology* **51**: 139–144.

McParland EL, Levine NM. 2019. The role of differential DMSP production and community composition in predicting variability of global surface DMSP concentrations. *Limnology and Oceanography* **64**: 757–773.

Meyer N, Bigalke A, Kaulfuß A, Pohnert G. 2017. Strategies and ecological roles of algicidal bacteria. *FEMS Microbiology Reviews* **41**: 880–899.

Mitsutani A, Takesue K, Kirita M, Ishida Y. 1992. Lysis of *Skeletonema costatum* by *Cytophaga* sp. Isolated from the Coastal Water of the Ariake Sea. *Nippon Suisan Gakkaishi* **58**: 2159–2167.

Paul C, Pohnert G. 2011. Interactions of the algicidal bacterium *Kordia algicida* with diatoms: regulated protease excretion for specific algal lysis. *PLoS ONE* **6**: e21032.

Sayers EW, Bolton EE, Brister JR, Canese K, Chan J, Comeau DC, Connor R, Funk K, Kelly C, Kim S *et al.* 2022. Database resources of the National Center for Biotechnology Information. *Nucleic Acids Research* **50**: D20–D26.

Schäfer H, Abbas B, Witte H, Muyzer G. 2002. Genetic diversity of 'satellite' bacteria present in cultures of marine diatoms. *FEMS Microbiology Ecology* **42**: 25–35.

Seyedsayamdost MR, Case RJ, Kolter R, Clardy J. 2011. The Jekyll-and-Hyde chemistry of *Phaeobacter gallaeciensis*. *Nature Chemistry* **3**: 331–335.

Shi X, Liu L, Li Y, Xiao Y, Ding G, Lin S, Chen J. 2018. Isolation of an algicidal bacterium and its effects against the harmful-algal- bloom dinoflagellate *Prorocentrum donghaiense* (Dinophyceae). *Harmful Algae* **80**: 72–79.

Shivaji S, Sathyanarayana Reddy G, Sundareswaran VR, Thomas C. 2015. Description of *Thalassospira lohafexi* sp. nov., isolated from Southern Ocean, Antarctica. *Archives of Microbiology* **197**: 627–637.

Sonnenschein EC, Phippen CBW, Bentzon-Tilia M, Rasmussen SA, Nielsen KF, Gram L. 2018. Phylogenetic distribution of roseobacticides in the Roseobacter group and their effect on microalgae. *Environmental Microbiology Reports* **10**: 383–393.

Suleiman M, Zecher K, Yücel O, Jagmann N, Philipp B. 2016. Interkingdom cross-feeding of ammonium from marine methylamine-degrading bacteria to the diatom *Phaeodactylum tricornutum*. *Applied and Environmental Microbiology* **82**: 7113–7122.

Tamura K, Stecher G, Kumar S. 2021. MEGA11: molecular evolutionary genetics analysis version 11. *Molecular Biology and Evolution* **38**: 3022–3027.

Taylor JD, Cottingham SD, Billinge J, Cunliffe M. 2014. Seasonal microbial community dynamics correlate with phytoplankton-derived polysaccharides in surface coastal waters. *ISME Journal* **8**: 245–248.

Taylor JD, Cunliffe M. 2016. Multi-year assessment of coastal planktonic fungi reveals environmental drivers of diversity and abundance. *ISME Journal* **10**: 2118–2128.

Teeling H, Fuchs BM, Becher D, Klockow C, Gardebrecht A, Bennke CM, Kassabgy M, Huang S, Mann AJ, Waldmann J *et al.* 2012. Substrate-controlled succession of marine bacterioplankton populations induced by a phytoplankton bloom. *Science* **336**: 608–611.

Turner S, Pryer KM, Miao VPW, Palmer JD. 1999. Investigating deep phylogenetic relationships among cyanobacteria and plastids by small subunit rRNA sequence analysis. *The Journal of Eukaryotic Microbiology* **46**: 327–338.

Van Tol HM, Amin SA, Armbrust E. 2017. Ubiquitous marine bacterium inhibits diatom cell division. *ISME Journal* **11**: 31–42.

Vernette C, Henry N, Lecubin J, de Vargas C, Hingamp P, Lescot M. 2021. The Ocean barcode atlas: a web service to explore the biodiversity and biogeography of marine organisms. *Molecular Ecology Resources* **21**: 1347–1358.

Wang H, Butt L, Rooks P, Khan F, Allen MJ, Ali ST. 2016. Characterisation of algicidal bacterial exometabolites against the lipid-accumulating diatom *Skeletonema* sp. *Algal Research* **13**: 1–6.

Widdicombe CE, Eloire D, Harbour D, Harris RP, Somerfield PJ. 2010. Long-term phytoplankton community dynamics in the Western English Channel. *Journal of Plankton Research* **32**: 643–655.

Yamamoto Y. 1978. Detection of algal lysing biological agents in lakes by the soft-agar overlayer technique. *Japanese Journal of Limnology* **39**: 9–14.

Zheng N, Ding N, Gao P, Han M, Liu X, Wang J, Sun L, Fu B, Wang R, Zhou J. 2018. Diverse algicidal bacteria associated with harmful bloom-forming *Karenia mikimotoi* in estuarine soil and seawater. *Science of the Total Environment* **631–632**: 1415–1420.

Supporting Information

Additional Supporting Information may be found online in the Supporting Information section at the end of the article.

Dataset S1 18S sequences amplified for *Chaetoceros* sp. PLY617 and *Skeletonema* sp. PLY627.

Dataset S2 Strains of bacteria isolated from plaque assays during this study.

Fig. S1 Schematic diagram of the environmental sampling pipeline used to systematically isolate diatom antagonistic bacteria from the Western English Channel.

Fig. S2 Maximum likelihood phylogenetic tree of 16S rRNA gene sequences from bacteria isolated from 65 plaques identified during this study.

Fig. S3 Light microscope image of an example plaque on a *Chaetoceros* plaque assay plate.

Fig. S4 Growth over time of five axenic diatom host species in co-culture with *Ponticoccus alexandrii*.

Fig. S5 *Ponticoccus alexandrii* is algicidal towards *Thalassiosira pseudonana*.

Fig. S6 Colonisation of *Thalassiosira pseudonana* cells by *Ponticoccus alexandrii*.

Fig. S7 Growth of the diatoms *Skeletonema* sp. PLY627 and *Thalassiosira weissflogii* in co-culture with different WEC plaque-forming bacteria.

Fig. S8 Environmental metadata collected at station L4 from June 2020 to July 2021.

Fig. S9 Abundance of diatoms of the genera *Skeletonema*, *Thalassiosira* and *Chaetoceros* as well as bacteria at L4 station from June 2020 to July 2021.

Fig. S10 Maximum likelihood phylogenetic tree of 16S rDNA sequences of *Thalassospira* species.

Fig. S11 Maximum likelihood phylogenetic tree of 16S rDNA sequences of *Maribacter* species.

Fig. S12 Maximum likelihood phylogenetic tree of 16S rDNA sequences of *Marinobacter* species.

Fig. S13 Maximum likelihood phylogenetic tree of 16S rDNA sequences of *Halomonas* species.

Fig. S14 Global distribution and abundance of metabarcodes resembling Western English Channel antagonists in the *Tara* Oceans 16S/18S rDNA miTAG metabarcode databases.

Fig. S15 Maximum likelihood phylogenetic tree of 18S V9 rDNA sequences of *Skeletonema* species.

Fig. S16 Maximum likelihood phylogenetic tree of 18S V9 rDNA sequences of *Chaetoceros* sp.

Methods S1 Bioinformatics assessment of the global biogeography of WEC bacterial antagonists and diatom co-occurrence.

Table S1 Diatom taxa examined in this study.

Table S2 Reinoculation of plaques picked from original environmental plaque assays enables propagation of plaques.

Table S3 List of metabarcodes identified in the TARA Ocean Barcode Atlas resembling 16S rDNA sequences of WEC bacterial isolates with verified antagonistic activity against diatoms.

Table S4 List of *Tara* stations the metabarcodes for the bacterial species described in Table S3 were identified.

Table S5 List of metabarcodes identified in the TARA Ocean Barcode Atlas resembling 18S rDNA V9 region of diatom hosts affected by bacterial antagonists described in Table S3.

Please note: Wiley is not responsible for the content or functionality of any Supporting Information supplied by the authors. Any queries (other than missing material) should be directed to the *New Phytologist* Central Office.